



# Micro-electrochemical DO sensor with ultra-micropore matrix fabricated with femtosecond laser processing successfully applied in on-line DO monitoring for yeast culture

Meng Fan · Zhen Gu · Wei Chen · HuiFeng Wang · YingPing Zhuang · Jianye Xia

Received: 4 July 2022 / Revised: 19 December 2022 / Accepted: 5 January 2023 / Published online: 28 January 2023  
© The Author(s), under exclusive licence to Springer Nature B.V. 2023

**Abstract** Accurate monitoring of dissolved oxygen (DO) is vital for aerobic fermentation process control. This work presents an autoclavable Micro-Dissolved oxygen Sensor (MDS) that can monitor real time DO. The proposed sensor is much cheaper to be manufactured (<\$35) and can be adapted to varying measurement environments. An ultra-micropore matrix was created using femtosecond laser processing technology to reduce flow dependency of probe signals. The validity of the proposed DO sensor was

verified by testing it under different DO levels. The result revealed consistency between the new designed sensor and a commercial DO sensor. The obtained sensitivity was  $-7.93 \mu\text{A}\cdot\text{L}\cdot\text{mg}^{-1}$  (MDS with ultra-micropore matrix). Moreover, the MDS can function without an oxygen-permeable membrane and a solid electrolyte was used which reduced the response time (4.6 s). For real-time monitoring, the stability of the MDS was validated during a yeast batch fermentation carried out until 18 h.

**Supplementary Information** The online version contains supplementary material available at <https://doi.org/10.1007/s10529-023-03348-0>.

M. Fan · Y. Zhuang · J. Xia (✉)  
State Key Laboratory of Bioreactor Engineering,  
East China University of Science and Technology,  
Shanghai 200237, China  
e-mail: xiajy@tib.cas.cn

Z. Gu · H. Wang  
Key Laboratory of Smart Manufacturing in Energy  
Chemical Process Ministry of Education, East China  
University of Science and Technology, Shanghai 200237,  
China

W. Chen  
XXL-The Extreme Optoelectromechanics Laboratory,  
School of Physics and Electronic Science, East China  
Normal University, Shanghai 200241, China

J. Xia  
Tianjin Institute of Industrial Biotechnology, Chinese  
Academy of Science, Tianjin 300308, China

**Keywords** All-solid electrolyte · Dissolved oxygen sensor · Electrolysis · Real time monitoring · Yeast fermentation

## List of symbols

$k_{DO}$	First order rate constant for DO probe model ( $\text{s}^{-1}$ )
$c_{l,O_2}$	Oxygen concentration near the surface of DO sensor
$c_{s,O_2}$	Oxygen concentration inside the sensor
$c_{DO}$	Output of the DO sensor
$\tau_e$	Response time
$I_{relative}$	Relative value of current to characterize flow dependence
$Current_{rpm_i}$	The measured current of sensors under different rotation speeds
$Current_{max \in rpm_i}$	The maximum current of $Current_{rpm_i}$
$X_{CO_2,out}$	Volume fraction of $CO_2$ in off-gas

$X_{CO_2,in}$	Volume fraction of CO <sub>2</sub> in off-gas
$X_{O_2,in}$	Volume fraction of O <sub>2</sub> in air
$X_{O_2,out}$	Volume fraction of O <sub>2</sub> in air
$F_{in}$ and $F_{out}$	Volumetric flow rate of inlet air and outlet off-gas under standard condition
$V_{broth}$	Volume of the broth in bioreactor

## Introduction

Dissolved oxygen (DO) is an important parameter for aerobic fermentation process in various bioreactors (Haiyuan et al. 2020; Hyunjin et al. 2017; Milica et al. 2006; Seyed Ali et al. 2016; Justin et al. 2020), as it plays a critical role in supporting the respiration of the culture of the microorganism in bioreactors. The level of DO in a bioreactor may often indicate the metabolic status of the microorganism. The development of small-scale bioreactors for high throughput strain screening and bioprocess optimization has been fast growing over more than two decades (Andrijana et al. 2016), and the volume of which ranges from a few milliliters to tens of milliliters (Buchenauer et al. 2009; Gabi et al. 2011; Michel et al. 2010). That requires that the size of the DO sensor should be small enough to fit in the miniature bioreactors. The advantage of commercialized macro-scale electrodes is that they are not prone to be interference by the problems associated with concentration differences, filling solution evaporation, thin film dissolution and liquid junction potentials. However, due to their bulky nature, they are harder to integrate into miniature biosensors (Tom and Bland 2008). There is an increasing trend towards miniaturization of both biological and chemical DO sensors for usage with miniaturized sample pre-processing and analysis systems (Tom and Bland 2008). Despite optical DO electrode is regarded as a better choice in the environmental water monitoring field (Andrijana et al. 2016; Tobias et al. 2013; Mário et al. 2013; Schmiderder et al. 2015), its application in fermentation field is restricted. Because fluorescence dye used in optical DO is high temperature sensitive and has problem to be autoclaved with high temperature and pressure, which is crucial for microorganism pure culture in bioreactor. The Clark cell remains the most reliable sensor to measure dissolved oxygen concentration but miniaturization is complicated. Since normal size macro DO electrode

mounted in stirred tank bioreactor, it might take up to several minutes before the DO concentration gradient to be in equilibrium and the resulting diffusion boundary layer is prone to be interfered by bulk convective flow. In conventional Clark oxygen sensors, these problems are circumvented by building up the concentration gradient mainly builds up in a membrane, which encloses the amperometric cell with an internal cavity. An effective way to overcome convective the flow interference of the current detection is by applying ultra-micropore matrix, which is a term generally denoting circular pores with a diameter below 5 µm covering the surface of the sensor (Eric et al. 2008) and the same effect with a diameter of 10 µm was proven in this article. Femtosecond (fs) laser has become a powerful tool for fabricating three-dimensional (3D) microstructures from nano-to-micron scale in transparent materials, which is enabled in either additive/subtractive manners or an internal modification fashion (Wei et al. 2019; Rafael and Eric 2008; Kazuyoshi et al. 2006; Koji and Ya 2014; Xiaolong et al. 2019). As a maskless technology, femtosecond laser enables rapid prototyping and provides a straightforward approach to fabricate 3D structures inside photosensitive materials, including polymer and glass (Anthony et al. 2016; Yang et al. 2012; Zijie et al. 2020; Jia et al. 2020; Gregor et al. 2019). It is possible to be used to make the microchannels for overcoming the convective flow interference problem.

In this study, we propose a micro-dissolved oxygen sensor (MDS) with a femtosecond laser fabricate ultra-micropore matrix structure, which is not sensitive to bulk convective flux interference. The proposed sensor replaces the liquid electrolyte with solid electrolyte, so that only-oxygen-permeable membrane is no longer required and the sensor can undergo high temperature sterilization. A precise electrochemistry instrument system was developed based on the new-designed sensor. The performance of the electrodes was tested in with a pure water system, which showed the good stability and repeatability of sensor signals, and no significant flow dependence was observed in the measured DO value. On the basis of cold flow model experiments, the sensor was applied in a real fermentation process in real-time and continuous measurement of DO for 18 h. The new designed Micro-DO sensor presented here showed shorter response times and lower costs than commercial DO

probes. More importantly, the small size of the sensor offers the potential to be used in more diverse environments with little adaption.

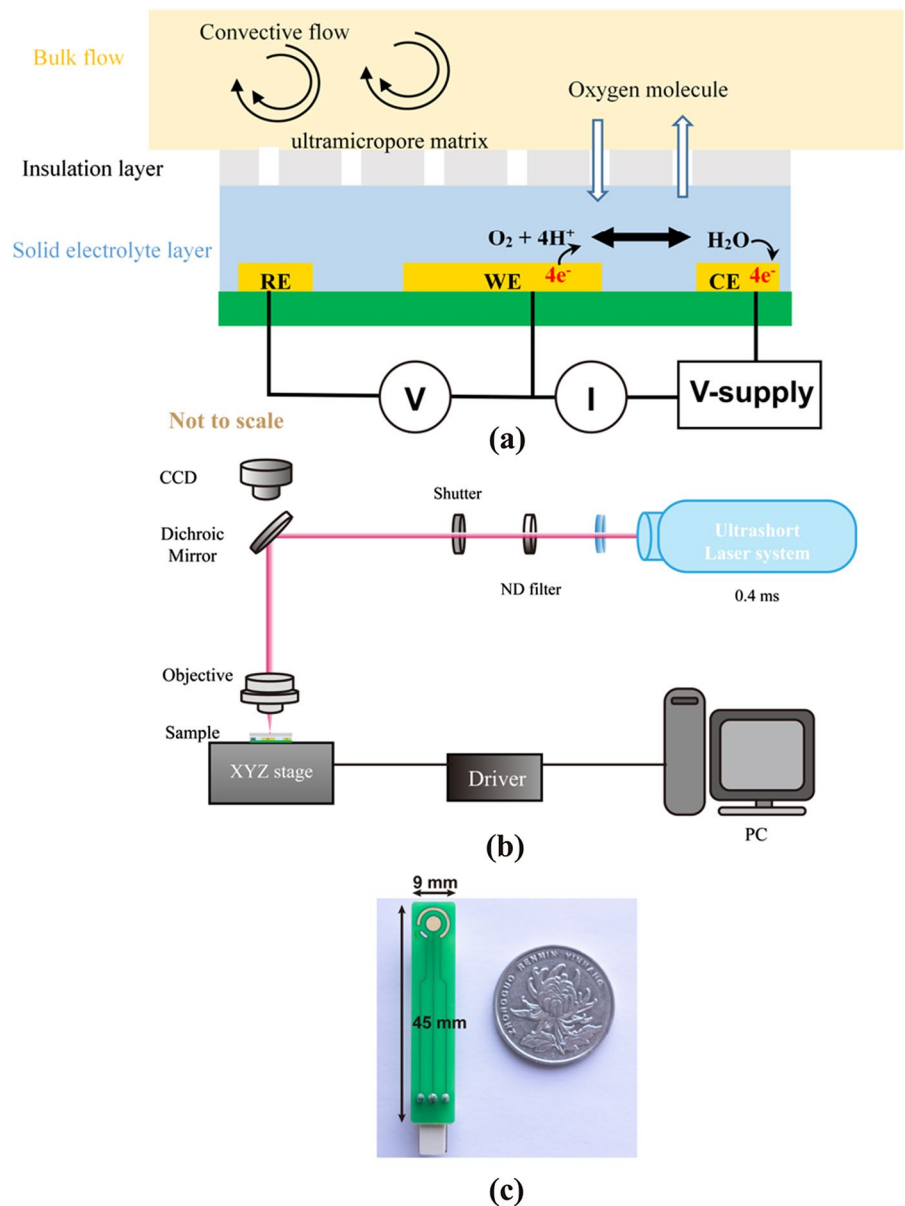
**Materials and methods**

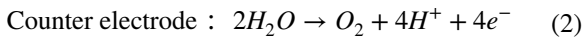
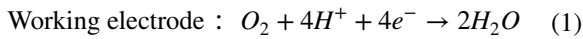
**Principle of the MDS**

Figure 1a shows the schematic structure of the MDS, which can be divided into three layers: the

three solid electrodes layer (Fig. 1c), solid electrolyte layer, and the top insulation layer with ultramicropores matrix generated using a femtosecond laser. The three electrodes in the DO sensor measure the current caused by reduction of dissolved oxygen in the solid electrolyte. The reduction reaction of the dissolved oxygen at the working electrode and that on counter electrode is described by the following Eqs. (1, 2) (Jungil et al. 2007):

**Fig. 1** Schematic diagram of the structure and manufacturing method for the new-designed micro-DO sensor. **a** Illustration of assembled DO sensor and a cross-sectional diagram of the chemical reaction for the Clark-type electrode. **b** Schematic diagram of femtosecond laser processing. **c** Physical image and size





### Fabrication of MDS

An MDS with three electrodes consists of an Au working electrode (3 mm in diameter), an Au counter electrode, and an Ag reference electrode as shown in Fig. 1b. Ni/Cu (20 nm/ 200 nm) layers were deposited onto a printed circuit board (PCB) using an Angstrom E-beam Evaporator (Angstrom Engineering Inc.), followed by deposition of Ag (250 nm) for the reference electrode (cost \$5). The probe was cleaned using 75% C<sub>2</sub>H<sub>5</sub>OH with 30 min ultrasonic processing and dried at 60 °C. After cleaning, a 300 mV constant voltage current source was applied to obtain Ag/AgCl reference electrode from the original Ag electrode. The cathode of the power supply was connected to the Ag electrode, and the anode of the power supply to Pt electrode and both electrodes were submerged in 0.1 M KCl solution for 15 s. A thin layer of Nafion solution (Sigma 117) was fabricated on the surface of the probe. The solvent was then dried by placing the electrode in a vacuum drying oven with 0.95 degrees of vacuum at 60 °C for 2 h. Epoxy resin was used as an insulating layer over the Nafion layer. The resin was evenly distributed on the electrode surface using a spin coater with 2.01 g (3000 rpm) and then solidified at 70 °C for 24 h. The resin layer was then processed to generate the ultra-micropore matrix using the femtoseconds laser as illustrated in Fig. 1b. An ultrashort laser system (Light Conversion, Pharos-20 W) with a central wavelength of 1028 ± 5 nm, a repetition rate of 2 kHz, and a variable pulse duration was employed for laser direct writing. The pulse energy of the laser beam was tuned using a variable neutral density filter. The pulse durations of the laser beam were set at 0.4 ms by moving a motorized translation stage to change a compressor length and induce a positive chirp and the pulse energies were set 6 μJ to make the proper ultra-micropores (cost less than \$10).

### Configuration of the whole measuring system

The instrument system signal processing to receive current data from MDS is designed based on a previous work (Zhen et al. 2018), which contains the electrode interface, analog front, microcontroller, data transceiver and multiplexer (cost \$15). The current on the working electrode is converted to voltage by using a trans-impedance amplifier (TIA) in the front end with selectable feedback resistance from 1 to 10 MΩ to adjust the measuring range through the multiplexer. Two on-chip DACs (12-bit) are used to control the potential for implementation of the cyclic voltammetry.

### Characterizations of the MDS

Several steady state DO levels were established in a 1.5-L beaker through the air and N<sub>2</sub> mixing with different ratios before the mixture enters into the solution. The Nafion MDSs were tested in double-distilled water (dd-water), 2.5–10% (w/w) of lactic acid, malic acid, citric acid, ethanol, respectively, and under different temperatures (15–55 °C) or different pH values (pH 0–14). The flow rates of air and N<sub>2</sub> were controlled by two mass flow meters. The DO value in the beaker was also measured with a commercial DO probe (VisiFerm DO Arc 120, Hamilton, Bonaduz, Switzerland) at the same time. Cyclic voltammetry was performed by sweeping linearly from – 300 mV to – 500 mV at a scan rate of 50 mV/s (Hyunjin et al. 2017). Then, the Nafion MDS were tested for their properties after high temperature sterilization (121 °C for 30 min, required for pure microorganism culture application) for 50 times.

### Dynamic response and flow dependence testing

Response time testing was carried out under fluctuating dissolved oxygen conditions. The fluctuating DO condition was created using a two-gas switching system, and the system consisted of two electromagnetic valves controlling the cutover of air and N<sub>2</sub> (99.999%) and one mass flow controller that fixes the flow rate of the gas to be under 1 vvm. Intermittent switching of nitrogen and air with a 5-min period cycle to achieve periodic changes in dissolved oxygen in a 5-L bioreactor (GuoQiang Company, Shanghai, China). During the process pH was kept at 5.0 ± 0.2 and the

temperature at  $30 \pm 0.5$  °C. A commercialized dissolved oxygen probe (VisiFerm DO Arc 120, Hamilton, Bonaduz, Switzerland) was mounted in the same system as a control to validating the new-designed probe. If we switch the electrode from one DO level ( $DO_1$ ) solution to another different DO level ( $DO_2$ ), a constant response time value ( $\tau_e$  assume a first order response kinetics) defined as the time needed for the probe signal reaches 63% of the difference ( $DO_2 - DO_1$ ) was obtained and the kinetics process can be expressed as (3) and (4) (Nulee et al. 2020) (de Jongea et al. 2014):

$$\frac{\partial c_{s,O_2}}{\partial t} = k_{DO}(c_{l,O_2} - c_{s,O_2}) \quad (3)$$

$$c_{DO}[t + \tau_e] = c_{s,O_2}[t] \quad (4)$$

The following procedure was used to obtain  $\tau_e$ . The designed DO sensor was initially put into a zero DO level solution sparged with pure  $N_2$  until the signal is steady. Switch the probe immediately to an oxygen saturated solution nearby, and the response curve of the probe signal was recorded. The switching time was neglectable as it is less than 0.5 s, which is much smaller than the response time of the electrodes.

The flow dependence of the different MDS was tested at a constant dissolved oxygen concentration (8.05 mg/L, at 25 °C and 1 atm). Rotation speed was increased gradually from 100 to 700 rpm in a period of 5 min and the same cyclic voltammetry was performed.

$$I_{relative} = \frac{Current_{rpm_i}}{Current_{max \in rpm_i}} \quad (5)$$

#### Preculture and batch cultivation of yeast

Preculture of *S. cerevisiae* B1 was carried out for 9 h in three 500 mL shake flasks with 100 mL working volume at 30 °C, and the batch cultivation served as inoculum for the 5-L bioreactor (GuoQiang Company, Shanghai, China) with a working volume of 3 L of mineral medium (Jianye et al. 2022). The pH was controlled at 5.0 with 3 M NaOH as titrate. The temperature of the batch was set at 30 °C also. Two Rushton turbine impellers were mounted for mixing and gas–liquid mass transfer with 200 rpm.

Sterilized air was sparged into the reactor with a flow rate of 3 L/min (1 vvm). The off-gas of the fermentation was analyzed using an off gas-MS (Prima BT, Thermo Fisher Scientific, Winsford, U.K.), and oxygen uptake rate (OUR), carbon dioxide evolution rate (CER) and respiratory quotient (RQ) were calculated based on the MS measured off-gas composition according to Eqs. (6) to (8). The bioreactor was operated with a gauge pressure of 0.05 MPa.

$$CER = \frac{X_{CO_2,out}F_{out} - X_{CO_2,in}F_{in}}{V_{broth}} \quad (6)$$

$$OUR = \frac{X_{O_2,in}F_{in} - X_{O_2,out}F_{out}}{V_{broth}} \quad (7)$$

$$RQ = \frac{CER}{OUR} \quad (8)$$

## Result and discussion

### Electrochemical response of MDS

Firstly, we tested the properties of the new-designed micro-DO electrode in a 1.5-L beaker. Figure 2a shows the dissolved oxygen levels under different steady state DO levels within around 80 min at room temperature and 1 atm pressure. The cyclic voltammetry (CV) measurements of the new-designed sensor under seven DO states are shown in Fig. 2b. Cathodic current demonstrated better linear current response in the potential range of  $-350$  mV to  $-450$  mV. As shown in Fig. 2c, the greatest regression coefficient under different voltage is at  $-400$  mV, so the  $-400$  mV current is chosen as the operating voltage. In Fig. 2d, we compared the regressed DO vs. electrode current lines for the new designed micro-DO probes with different setups. It can be seen that the probes with ultra-micropore matrix structure obtains the best regression line with an excellent correlation coefficient ( $R^2 = 0.9939$ ). In the actual fermentation process, the fermentation broth is complex in composition and may contain various metabolites, like alcohols, organic acids, etc. In addition, different level of temperature and pH may be required for different strains. Therefore, the validity of the Nafion MDSs were tested under various conditions mentioned

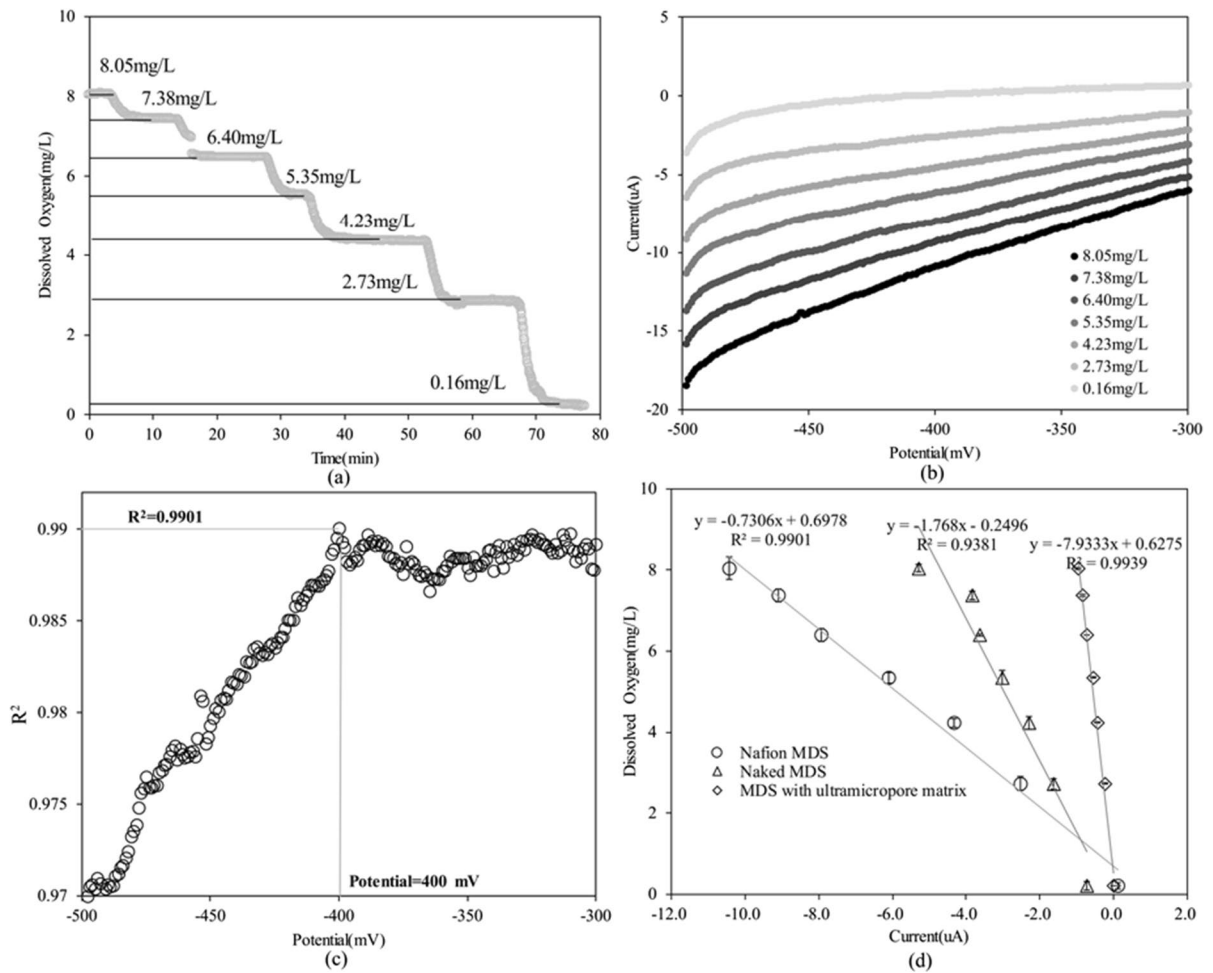


**Fig. 2** Cold flow model testing of the properties of the new designed Micro-DO sensor. **a** 7 different DO concentration levels. **b** Cyclic voltammetry of Nafion MDS. **c** Distribution

of regression coefficients for different voltages. **d** Influences on calibration curve of 3 different processes MDS

above. In the presence of organic acids or ethanol and with pH changes, the Nafion MDSs show consistent linearity for different dissolved oxygen concentrations (Supplementary Fig. 1a–e). According to the ANOVA analysis, the slopes and intercepts obtained in the above cases were not significantly different from those tested in pure water ( $P > 0.05$ , Fig. 3). At constant air pressure, the solubility of insoluble gases in water decreases with increasing temperature. As a result, the measured current also decreases with increasing temperature (Supplementary Fig. 1f). To confirm the reliability of the sensors after sterilization, the Nafion MDSs were sterilized 50 times and tested after each 5 autoclaves (Supplementary

Fig. 2). According to the ANOVA analysis, the slopes keep no significant changes and the intercepts were not changed significantly after 25 times autoclaves (Fig. 4b, Table 1).

#### Dynamic and flow dependence results

The response time of the DO probe is required to be as small as possible in order to catch the oxygen uptake kinetics of the cell within the system, which is attributed to the low solubility of oxygen (0.26 mmol/L at 25 °C and 1 atm) (Xiao et al. 2019) in fermentation broth under normal condition (at 25 °C and 1 atm) and relative higher oxygen uptake rate

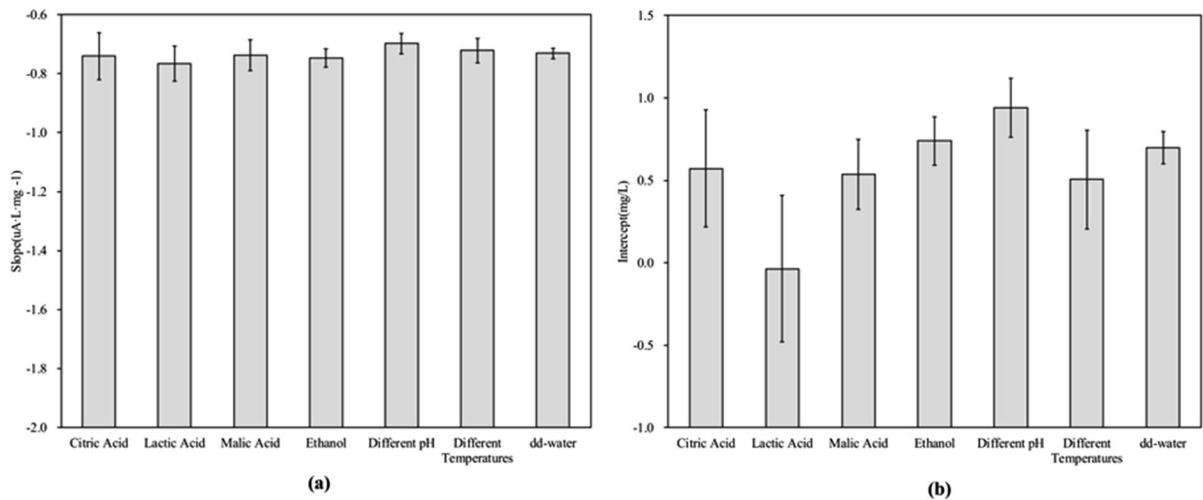


**Fig. 3** Variations of **a** slopes and **b** intercepts under various relevant conditions for testing the Nafion MDS

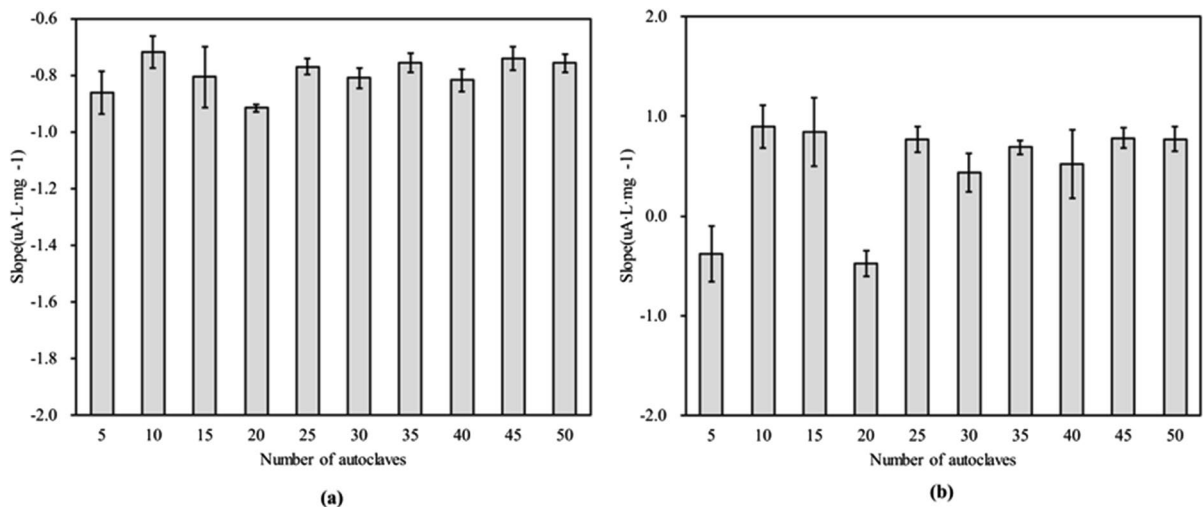


**Fig. 4** Variations of **a** slopes and **b** intercepts after every 5 times autoclaves for a total of 50 times autoclaves

of yeast cells in bioreactor (normally over 60 mmol/L/h when biomass OD600 is over 40) (Zhiqiang et al. 2008).

The response time of Clark-type sensors is affected by some elements, such as membrane type, membrane thickness, area of the working electrode and a gap between the membrane and the working electrode surface (Lee and Kim 2004). Compared to the commercial electrodes used in this work, the proposed electrode uses a solid electrolyte with a layer total thickness of less than 2  $\mu\text{m}$ . This special structure

improvement reduces the distance between bulk dissolved oxygen molecule and the electrode where oxygen molecules are reduced, and in turn it reduces also the response time of the probe. A schematic diagram of the measurement process is shown in Fig. 5a. Figure 5b shows the profile of measured DO level using the new designed micro-electrode in three full cycles of air-nitrogen intermittent shifting within approximately 30 min. Raw current data of the probe showed a deviation of 1.79% at dissolved oxygen saturation versus zero dissolved oxygen. The data in Fig. 5b

**Table 1** Table of the differences of profiles' slopes and intercepts after 5–50 autoclaves

Number of auto-claves	Average slope	Average intercept	Std.slope	Std.intercept
5	−0.86	−0.38	0.08	0.28
10	−0.72	0.90	0.06	0.21
15	−0.81	0.84	0.11	0.34
20	−0.92	−0.48	0.01	0.13
25	−0.77	0.77	0.03	0.13
30	−0.81	0.44	0.04	0.19
35	−0.76	0.69	0.03	0.07
40	−0.82	0.52	0.04	0.35
45	−0.74	0.78	0.04	0.10
50	−0.76	0.77	0.03	0.12

shows that it requires 100 s from zero dissolved oxygen to 90% of saturated dissolved oxygen and needs more 100 s to 100% due to the reduction of the oxygen concentration difference between the gas and liquid phases. The long conversion time of 200 s does not mean that the electrodes have a long response time. Because the complete elimination of  $N_2$  in the reactor often needs at least five residence times, corresponding to about 3.3 min. However, the information of the probe response time  $\tau_e$  contained in the response time of the DO profile. The response time of the commercialized DO probe and the new-designed micro-DO sensors were measured (The response curve of the probe signals is shown in Fig. 5c). The corresponding response time  $\tau_e$  is 10.2 s and 4.6 s for commercial sensor and the MDS, respectively. For the vast majority of application scenarios, a response time of 10.2 s is sufficient, because a fermentation often runs from a few days to several weeks. However, for certain conditions where dissolved oxygen changes more rapidly, we believe that a shorter reaction time should be beneficial. Variety of different pulse experiments were carried out, e.g. sugar pulse (Peng et al. 2021), oxygen pulse (Diano et al. 2006) and ethanol pulse (Diana et al. 2004) experiments were designed to study the properties of microorganism oxygen uptake kinetics, in which cases rapid dynamic changes of DO accompanied. A shorter  $\tau_e$  is thus crucial for obtaining real-time dissolved oxygen level and the accurate property of the microorganism. A shorter response time of the new designed micro probe makes it much easier for achieving this purpose.

Some researchers used the method of ultra-micropore matrix to overcome the problem of the

influence of convective flow to the probe signal (Eric et al. 2008), in this case, the equilibrium oxygen concentration profile builds up within a few milliseconds, and the contribution of diffusion to the total mass transfer of oxygen becomes so high that it is hardly influenced by convection flow. Two kinds of laser fabrication methods were tested: ULS laser platform (VLS2.30 Universal, America) and a femtosecond laser amplifier (Libra, Coherent, Inc.). Figure 3d shows the aperture formed by  $CO_2$  laser cutting are irregular and non-uniform ( $118.9 \pm 42.3 \mu m$ ). The pictures shot by stereomicroscope (SZX16, Olympus Corporation, Japan) are 8 times (center) and 40 times (around) respectively. In contrast, the ultra-micropore matrix generated by femtosecond laser shown in Fig. 5e is much more regular with pore diameter of 10  $\mu m$  and inter-pore distance of 50  $\mu m$  and about 50 thousand pores covered RE, WE and CE. We compared the resistance of probe signal to the convective flow for the new designed probe with different processing method, and the result is shown in Fig. 5f. All experiments were conducted under a saturated dissolved oxygen condition (8.05 mg/L, at 25 °C and 1 atm) to ensure that the dissolved oxygen did not change with impeller rotation speed. The raw currents in the probe are logged during the process, and the  $I_{relative}$  gradually increased as the rotational speed increasing for both MDS without the resin layer and laser cutting MDS. However,  $I_{relative}$  of MDS with ultra-micropore matrix on the resin layer fabricated by the femtosecond laser showed stability during the whole process (standard deviation is within  $\pm 5\%$ ).



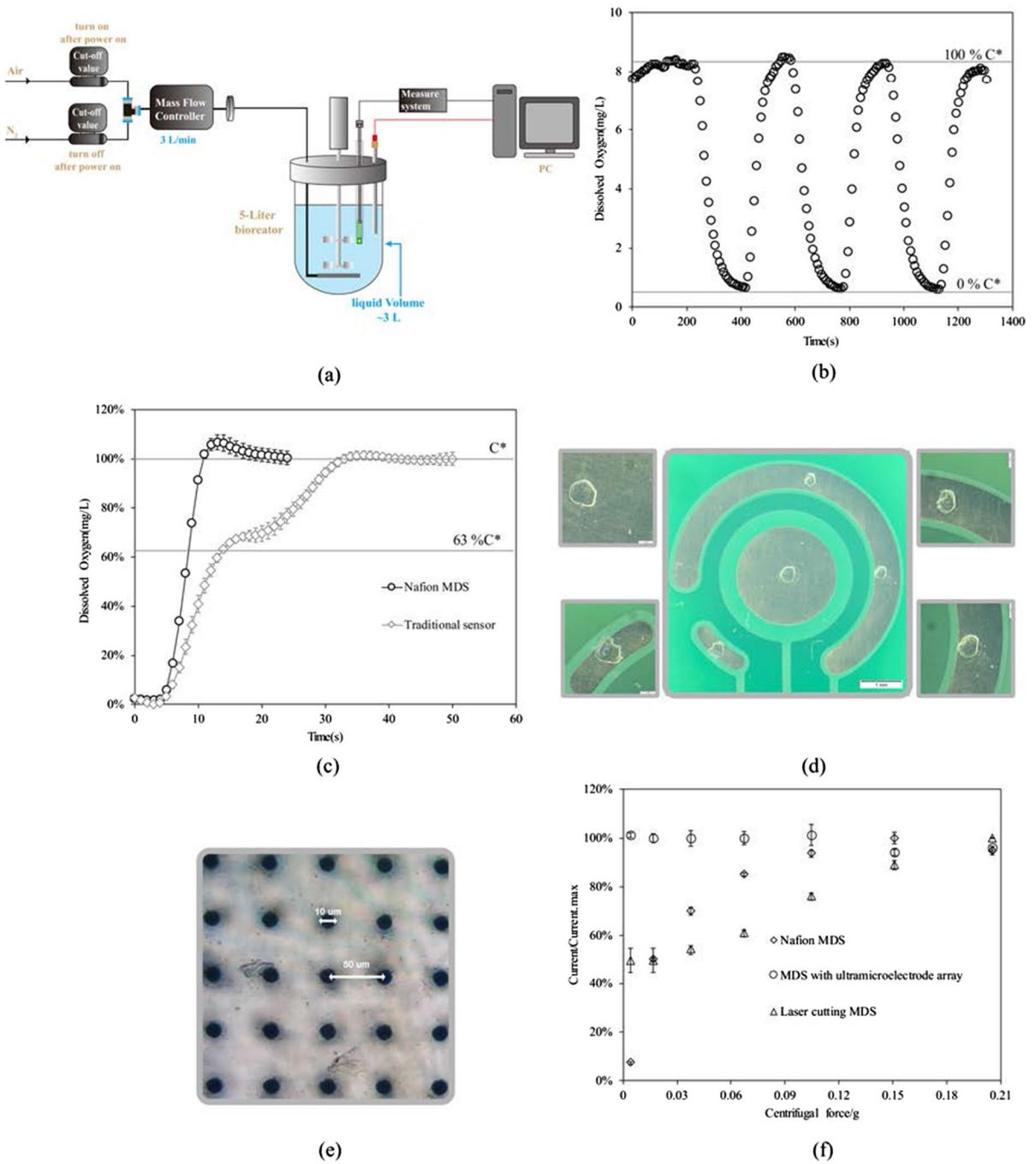


**Fig. 5** Response and convective flow interference testing of the new designed micro-DO sensor. **a** Schematic diagram of cold model test in 5-L bioreactor. **b** Testing at dynamic state.

**c** Definitions of  $\tau_e$  for commercial sensor and Nafion MDS. **d** Structure of ultra-microelectrodes. **e** Holes made by CO<sub>2</sub> laser cutting. **f** Flow dependence test of Nafion MDS

## Dissolved oxygen measurement results of the yeast batch culture

The MDS was applied to batch yeast fermentation in a 5-L bioreactor (GuoQiang Company, Shanghai, China) to verify the stability and feasibility of the new designed micro-DO sensor in real fermentation conditions for monitoring the process DO. The real fermentation broth system has a rather complex environment, which proposes a challenge to the use of microelectrodes. Living cells and metabolites,

complex gas-and liquid two-phase turbulence flow make the measurement of DO level a challenging work. It is therefore necessary to validate the micro-electrodes applicability in a real fermentation process for accurate DO measurements. During the batch cultivation the dissolved oxygen concentration decreased with time due to the increasing oxygen demand of the exponentially growing yeast. Figure 6a shows the installment of the MDS in the 5-L bioreactor. The batch experiments finished at approximately 18 h after inoculation. As can be seen in Fig. 6b, the batch

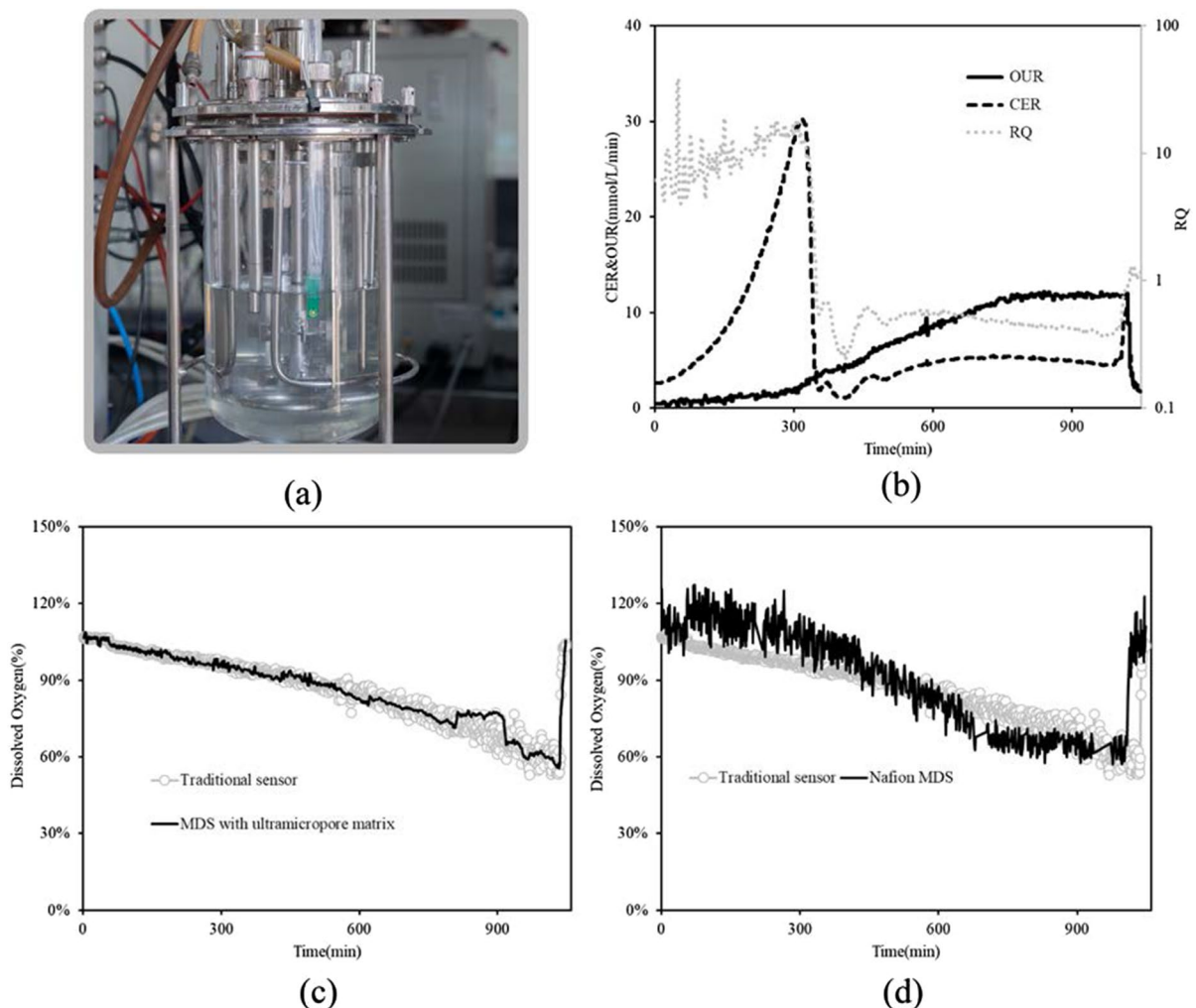


**Fig. 6** Application of new designed probe in a 5-L bioreactor with real fermentation process. **a** Mount of the new designed probe in a 5-L bioreactor; **b** Profiles of oxygen uptake rate (OUR), carbon dioxide evolution rate (CER) and respiration quotient (RQ) of the yeast cell culture process in the 5-L bio-

reactor; **c** Comparison between the dissolved oxygen signals from the conventional sensor and MDS with ultra-micropore matrix. **d** Comparison between the dissolved oxygen signals from the conventional sensor and Nafion MDS

fermentation of yeast shows two distinct phases due to the Crabtree effect of the yeast cell (Jianye et al. 2022). From 0 to 6.5 h (phase I, respire-fermentative state), yeast cells preferentially use the glucose as the carbon source and ethanol accumulated due to the high specific growth rate ( $>0.28 \text{ h}^{-1}$ ), indicating by a higher RQ value ( $>1$ ) during this phase. The yeast produces large quantities of ethanol for balancing the requirement of constant redox condition in the cytoplasm and support the higher ATP requirement for fast cell growth. From 6.5 to 18 h (Phase II), the cells started to utilize the accumulated ethanol after the glucose depleted in phase I, indicated by the decreasing of RQ from much larger than 1 to less than 1. The DO drops from 100 to 55% during the entire fermentation cycle and returns to 100% at the end of the fermentation. The micro-DO sensor was calibrated using two points calibration method (0% for zero dissolved oxygen and 100% for saturated dissolved oxygen concentration of 12.1 mg/L) before the batch cultivation. It can be seen in Fig. 6c that the new designed MDS's signal matched the signal of the commercial DO sensor (VisiFerm DO Arc 120, Hamilton, Bonaduz, Switzerland). Nafion MDS covered with only solid electrolyte but without the ultra-micropores matrix of resin layer was also tested under the same fermentation process. The signal of this probe was much prone to noise compared to that with the ultra-micropore matrix resin layer probe in Fig. 6d. This again verified that without the outer resin layer the raw current signal was very easy to be interfered by noises, such as convective flow, electromagnetic signals, etc. A way to improve the signal to noise ratio would be increasing the electrode area and thus the measured current. Covering the naked probe with solid electrolyte significantly increases the voltage measured by the CV, which helps to increase the signal-to-noise ratio. Roughly 10 h after inoculation, however, the sensitivity of the naked probe suddenly decreased, but this was not observed for MDS with ultra-micropore matrix resin layer.

## Conclusion

In conclusion, we proposed and fabricated a novel micro-DO sensor. It can be utilized in a wide range of bioreactors from milliliter scale to industrial scale composed to the traditional commercialized

DO probes. The slopes keep no significant change after 50 times autoclaves and the intercept was not changed significantly after 25 times autoclaves. The new designed probe adopted solid electrolyte rather than liquid electrolyte, which ensured a much shorter response time (4.6 s), in addition, we also found a proper process procedure that can significantly reduce the convective flow interference to the raw current signals of the probe. The miniature sensor is more economical to manufacture (less than \$35), easier to prepare, and it can suit more variable measurement environments. Femtosecond laser processing technology was used for the first time to manufacture ultra-micropores matrix with 10  $\mu\text{m}$  diameters and reduce flow dependence. The obtained sensitivity was  $-7.93 \pm 0.12 \text{ uA}\cdot\text{L}\cdot\text{mg}^{-1}$  for the new designed MDS with ultra-micropore matrix, showing an excellent performance ( $R^2 = 0.9939$ ). Preliminary experimental data showed that the MDS exhibit stability during an 18-h yeast fermentation. For longer-term biological processes, these manifestations should be further investigated.

**Supporting Information** Supplementary Figure 1—Validation of the Nafion MDS under (a) 2.5–10 % Citric acid; (b) 2.5–10 % Lactic acid; (c) 2.5–10 % Malic acid; (d) 2.5–10 % Ethanol; (e) pH 0–14; (f) 15–55 °C.

Supplementary Figure 2—Linear characterizations of sensors every 5 times autoclaves for a total of 50 times autoclaves.

**Author contributions** All authors contributed to the study conception and design. Specific contributions are as follows: Conceptualization and writing—review and editing, XJ and ZY; methodology, FM and CW; writing—original draft preparation, FM; software and hardware, GZ and WH. All authors have read and agreed to the published version of the manuscript.

**Funding** This work was financially supported by the National Key Research and Development Program of China (Grant No. 2021YFC2101100).

**Data availability** The datasets generated during and/or analyzed during the current study are available from the corresponding author on reasonable request.

## Declarations

**Competing interests** The authors declare that they have no competing interests.

**Ethical approval** This article does not contain any studies with human participants or animals performed by any of the authors.

## References

- Andrijana B, Hilde L et al (2016) A flexible well-mixed milliliter-scale reactor with high oxygen transfer rate for microbial cultivations. *Chem Eng J* 303:655–666. <https://doi.org/10.1016/j.cej.2016.05.117>
- Anthony KA, Wilson H et al (2016) 3D-printed microfluidics. *Angew Chem Int Ed* 55(12):3862–3881. <https://doi.org/10.1002/anie.201504382>
- Buchenaer A, Hofmann MC et al (2009) Micro-bioreactors for fed-batch fermentations with integrated online monitoring and microfluidic devices. *Biosens Bioelectron* 24(5):1411–1416. <https://doi.org/10.1016/j.bios.2008.08.043>
- de Jongea LP, Heijne JJ, van Guilk WM (2014) Reconstruction of the oxygen uptake and carbon dioxide evolution rates of microbial cultures at near-neutral pH during highly dynamic conditions. *Biochem Eng J* 84:42–54
- Diana V, Gertan A, van Z et al (2004) Analysis of in vivo kinetics of glycolysis in aerobic *Saccharomyces cerevisiae* by application of glucose and ethanol pulses. *Biotechnol Bioeng* 88(2):157–167. <https://doi.org/10.1002/bit.20235>
- Diano A, Bekker-Jensen S et al (2006) Polyol synthesis in *Aspergillus niger*: influence of oxygen availability, carbon and nitrogen sources on the metabolism. *Biotechnol Bioeng* 94(5):899–908. <https://doi.org/10.1002/bit.20915>
- Eric EK, van Leeuwen M et al (2008) A integrated electrochemical sensor array for on-line monitoring of yeast fermentations. *Biotechnol Bioeng* 99:884–892
- Gabi G, Ralf H et al (2011) A new microfluidic concept for parallel operated milliliter-scale stirred tank bioreactors. *Biotechnol Prog* 27(3):684–690. <https://doi.org/10.1002/btpr.570>
- Gregor W, Aleksandr O, Perdo F C (2019) Functional 3D printing for microfluidic chips. *Adv Mater Technol* 4(10):1900275. <https://doi.org/10.1002/admt.201900275>
- Haiyuan G, Michael S et al (2020) Applications of off-gas mass spectrometry in fed-batch mammalian cell culture. *Bioprocess Biosyst Eng* 43(3):483–493. <https://doi.org/10.1007/s00449-019-02242-2>
- Hyunjin L, Hyoungmin K et al (2017) Fabrication and characterization of micro dissolved oxygen sensor activated on demand using electrolysis. *Sens Actuators B Chem* 241:923–930. <https://doi.org/10.1016/j.snb.2016.10.145>
- Jia Q, Wenbo L et al (2020) A microfluidic mixer of high throughput fabricated in glass using femtosecond laser micromachining combined with glass bonding. *Micromachines* 11(2):213
- Jianye X, Benjamin JS et al (2022) Proteome allocations change linearly with the specific growth rate of *Saccharomyces cerevisiae* under glucose limitation. *Nat Commun* 13(1):2819. <https://doi.org/10.1038/s41467-022-30513-2>
- Justin MS, Luke AB et al (2020) Electrochemical dissolved oxygen sensor-integrated platform for wireless in situ bioprocess monitoring. *Sens Actuators b: Chem*. <https://doi.org/10.1016/j.snb.2020.128381>
- Jungil P, Jong-hyeon C et al (2007) Microfabricated Clark-type sensor for measuring dissolved oxygen. *IEEE*. <https://doi.org/10.1109/ICSENS.2007.4388677>
- Kazuyoshi I, Wataru W et al (2006) Ultrafast processes for bulk modification of transparent materials. *MRS Bull* 31(8):620–625. <https://doi.org/10.1557/mrs2006.159>
- Koji S, Ya C (2014) Ultrafast lasers—reliable tools for advanced materials processing. *Light Sci Appl* 3(4):e149–e149. <https://doi.org/10.1038/lsa.2014.30>
- Lee JH, Kim TJ (2004) A study on oxygen permeability of polypropylene membranes and their temperature dependency using medical oxygen sensor. *Ksbb J* 19(1):62–66
- Mário APN, Pedro CBF, Maria HLR (2013) Microtiter plates versus stirred mini-bioreactors in biocatalysis: a scalable approach. *Bioresour Technol* 136:30–40. <https://doi.org/10.1016/j.biortech.2013.02.057>
- Michel VL, Eric EK et al (2010) Aerobic batch cultivation in micro bioreactor with integrated electrochemical sensor array. *Biotechnol Prog* 26(1):293–300. <https://doi.org/10.1002/btpr.315>
- Milica R, Jos Malda et al (2006) Oxygen gradients correlate with cell density and cell viability in engineered cardiac tissue. *Biotechnol Bioeng* 93(2):332–343
- Nulee J, Mungyu L et al (2020) Behavior of CO-water mass transfer coefficient in membrane sparger-integrated bubble column for synthesis gas fermentation. *Bioresour Technol* 311:123594. <https://doi.org/10.1016/j.biortech.2020.123594>
- Peng L, Shuai W et al (2021) Dynamic response of *Aspergillus niger* to periodical glucose pulse stimuli in chemostat cultures. *Biotechnol Bioeng* 118(6):2265–2282. <https://doi.org/10.1002/bit.27739>
- Rafael RG, Eric M (2008) Femtosecond laser micromachining in transparent materials. *Nat Photonics* 2(4):219–225. <https://doi.org/10.1038/nphoton.2008.47>
- Schmidröder A, Severien T et al (2015) A novel milliliter-scale chemostat system for parallel cultivation of microorganisms in stirred-tank bioreactors. *J Biotechnol* 210:19–24. <https://doi.org/10.1016/j.jbiotec.2015.06.402>
- Seyed Ali MS, Fabio de F et al (2016) A microfluidic optical platform for real-time monitoring of pH and oxygen in microfluidic bioreactors and organ-on-chip devices. *Biomicrofluidics* 10(4):044111. <https://doi.org/10.1063/1.4955155>
- Tobias K, Konstantin S, Elmar H (2013) A system of miniaturized stirred bioreactors for parallel continuous cultivation of yeast with online measurement of dissolved oxygen and off-gas. *Biotechnol Bioeng* 110(2):535–542. <https://doi.org/10.1002/bit.24633>
- Tom F, Bland F (2008) Oxygen and the spatial structure of microbial communities. *Biol Rev Camb Philos Soc* 83(4):553–569. <https://doi.org/10.1111/j.1469-185X.2008.00054.x>
- Wei C, Peng W et al (2019) High-resolution femtosecond laser 3D micromachining using low-NA focusing systems (Vol. 10908). SPIE
- Xiao L, Cong H et al (2019) High cell density culture of baker's yeast FX-2 based on pH-stat coupling with respiratory quotient. *Biotechnol Appl Biochem* 66(3):389–397. <https://doi.org/10.1002/bab.1735>
- Xiaolong L, Jian X et al (2019) Polarization-insensitive space-selective etching in fused silica induced by picosecond laser irradiation. *Appl Surface Sci* 485:188–193. <https://doi.org/10.1016/j.apsusc.2019.04.211>

- Yang L, Jiangxin S et al (2012) Rapid prototyping of three-dimensional microfluidic mixers in glass by femtosecond laser direct writing. *Lab Chip* 12(4):746–749. <https://doi.org/10.1039/c2lc21015k>
- Zhen G, Huixin L et al (2018) A thumb-size electrochemical system for portable sensors. *Analyst* 143(12):2760–2764. <https://doi.org/10.1039/c8an00645h>
- Zhiqiang X, Meijin G et al (2008) Real-time viable-cell mass monitoring in high-cell-density fed-batch glutathione fermentation by *Saccharomyces cerevisiae* T65 in industrial complex medium. *J Biosci Bioeng* 105(4):409–413. <https://doi.org/10.1263/jbb.105.409>
- Zijie L, Jian X et al (2020) Freeform microfluidic networks encapsulated in laser-printed 3D macroscale glass objects.

*Adv Mater Technol* 5(2):1900989. <https://doi.org/10.1002/admt.201900989>

**Publisher's Note** Springer Nature remains neutral with regard to jurisdictional claims in published maps and institutional affiliations.

Springer Nature or its licensor (e.g. a society or other partner) holds exclusive rights to this article under a publishing agreement with the author(s) or other rightsholder(s); author self-archiving of the accepted manuscript version of this article is solely governed by the terms of such publishing agreement and applicable law.